# A Higgs-like Particle of 125 GeV from $H \to ZZ \to 4l$ Search

Yongao Hu*
*MIT Department of Physics*
(Dated: April 3, 2025)

This report presents an excess in signal of a Higgs-like particle around 125 GeV in the $H \to ZZ \to 4l$ search. The data is collected from the 2011 and 2012 LHC run at $\sqrt{s} = 7$ TeV and 8 TeV respectively. The results are consistent with the Standard Model prediction of a Higgs-like particle with a mass of 125 GeV, with a significance of 2.33 $\sigma$.

## I. INTRODUCTION

Higgs boson and the corresponding Higgs mechanism are the key components of the Standard Model of particle physics (SM). The Higgs boson is responsible for giving masses to the W and Z bosons, as well as fermions. The discovery of the Higgs boson at the Large Hadron Collider (LHC) in 2012 is one of the most important achievements in particle physics in the past decade [7]. This paper aims to reproduce the H→ZZ search in [7] and analyze the data collected by CMS experiments from the 2011 and 2012 LHC run at $\sqrt{s} = 7$ TeV and 8 TeV respectively to search for a Higgs-like particle with a mass of 125 GeV.

## II. THEORETICAL BACKGROUND

### II.1. Higgs Bosons

Higgs boson, a spin-0 massive particle, is a key component of SM. The corresponding Higgs field is a scalar field that permeates all of spacetime, and its non-zero vacuum expectation value (vev) leads to electroweak symmetry breaking, which gives masses to the W and Z bosons [17, 20]. Chiral fermions such as the matter content in SM also acquire mass through their interaction with the Higgs field [17, 20].
The Higgs boson is produced in high-energy collisions, such as those at the LHC [7]. The decay channels of the Higgs boson include H→ZZ, H→WW, H→bb, and H→$\tau\tau$ [10, 15].

### II.2. H→ZZ Decay

The decay of the Higgs boson into two Z bosons (H→ZZ) is a rare process, with a branching ratio of about 2.5% for a Higgs boson mass of 125 GeV [15]. The decay products of the Z bosons can be reconstructed from their decay into four leptons ($e^+e^-$ or $\mu^+\mu^-$). The final state consists of four charged leptons, which can be used to reconstruct the mass of the Higgs boson. The decay of the Z bosons into two charged leptons ($Z \to ll$) provides a clean signature for the Higgs boson search. This is because the products are non-hadronic, and there are no neutrino produced. The mass of the Higgs boson can be reconstructed from the invariant mass of the four-lepton system.

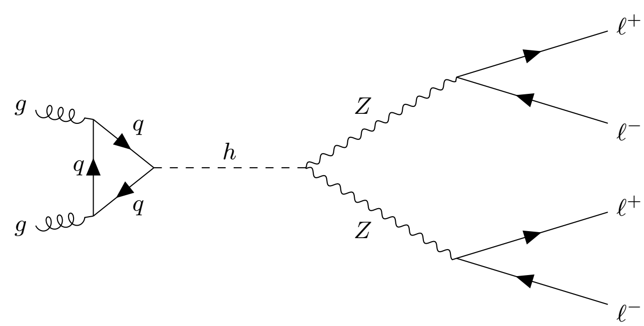


FIG. 1. Feynman diagram for the Higgs boson decay into two Z bosons and 4 leptons. The gluon fusion process is shown, where the Higgs boson is produced through a top or bottom quark loop. The gluons are produced when two protons collide with each other.

## III. BACKGROUND EVENTS

Nevertheless, there are several background processes that are irreducible, meaning that they mimic the signal and cannot be completely removed by selection criteria. The largest background is the continuum $ZZ^*$ production, which can mimic the signal. Some of the production processes are shown in Figure 2.
Besides, there are additional backgrounds from the production from Drell-Yan process, a QCD process that produces a pair of leptons from the annihilation of quarks and antiquarks, and $t\bar{t}$ production, which is the pair production of top and anti-top quarks that decays into leptons. These processes can also produce events that mimic the signal, but they are less significant than the continuum ZZ* production.

## IV. EXPERIMENTAL BACKGROUND

LHC is a proton-proton collider located at CERN, Geneva, Switzerland [7]. The LHC is the largest and

* yongao@mit.edu

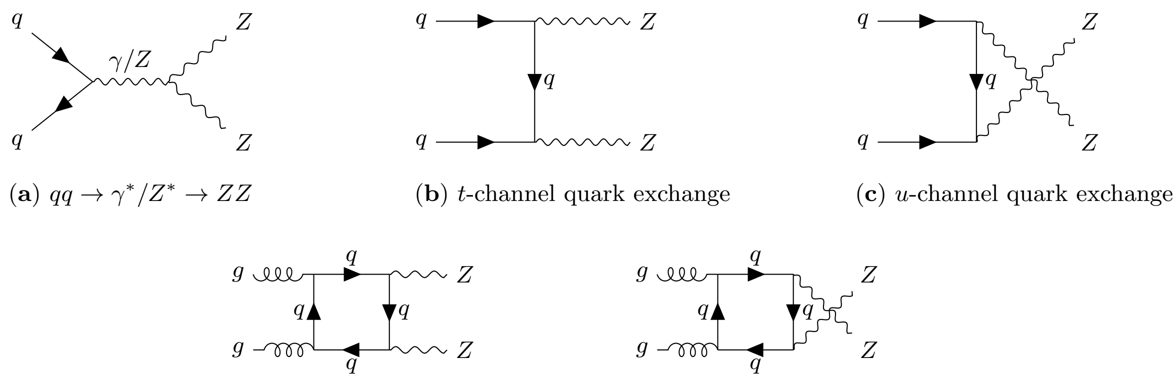


(**a**) $qq \to \gamma^*/Z^* \to ZZ$ (**b**) $t$-channel quark exchange (**c**) $u$-channel quark exchange

(**d**) $gg \to ZZ$ box diagram (**e**) $gg \to ZZ$ box diagram (crossed)

FIG. 2. Representative Feynman diagrams for continuum $ZZ^*$ production: (a)–(c) from quark–antiquark initial state, (d)–(e) from gluon–gluon initial state.

most powerful particle accelerator in the world, with a design energy of 14 TeV. The CMS experiment is a general-purpose detector designed to study a wide range of physics processes, including Higgs boson searches.

### IV.1. CMS Detector

CMS experiment includes a superconducting solenoid that provides a magnetic field of 3.8 T, a silicon tracker to measure the momenta of charged particles, a lead tungstate crystal electromagnetic calorimeter (ECAL) to measure the energy of photons and electrons, a brass/scintillator hadron calorimeter (HCAL) to measure the energy of hadrons, and gas-ionization muon detectors [7].

Pseudorapidity $\eta = -\ln(\tan(\frac{\theta}{2}))$, where $\theta$ is the polar angle from the positive $z$-axis, is used to describe the angular distribution of particles in the CMS detector. The silicon tracker tracks charged particles within the pseudorapidity range of $|\eta| < 2.5$. The ECAL and HCAL measures particles within the pseudorapidity range of $|\eta| < 3.0$. The muon detectors detect muons within the pseudorapidity range of $|\eta| < 2.4$.

### IV.2. Monte Carlo Simulation

The signal and background processes are generated using GEANT4 [1], POWHEG [3], PYTHIA 6.4 [19], and MadGraph 5 [4]. The choice parton distribution function (PDF) follows PDF4LHC working group recommendation [2, 5, 6, 13]. The simulation data is obtained from CMS Open Data [8, 11, 14].

## V. SELECTION CRITERIA

### V.1. Preliminary Selection

The data from [11, 14] has been pre-processed to remove the events that do not pass the preliminary selection criteria. The events are selected based on the following criteria:

- The events contains only four leptons, which are either electrons or muons as the final state particles.
- Transverse impact parameter with respect to the primary vertex $|d_{xy}| < 0.5$ cm.
- Longitudinal impact parameter with respect to primary vertex $|d_z| < 1$ cm.
- 3D impact parameter significance: $|\mathrm{SIP}| < 4$, where $\mathrm{SIP} = \frac{I}{\sigma_I}$, $I$ is the 3D lepton impact parameter, and $\sigma_I$ is its uncertainty. This ensures that the lepton pairs from Z boson decays originate from the same primary vertex.
- Muon and electron selection criteria: relative isolation of the lepton (reIso), the scalar sum of the transverse momenta of particles reconstructed within a distance $\Delta R$ of the object, normalized to the $p_T$ of the object, is smaller than 0.4 within a cone $\Delta R = 0.4$, where $\Delta R = \sqrt{(\Delta\eta)^2 + (\Delta\phi)^2}$. $\Delta\eta$ is the difference in pseudorapidity, and $\Delta\phi$ is the difference in azimuthal angle.

We further apply the following selection criteria to select the events that pass the preliminary selection [7]:

- Pseudorapidity of the lepton: $|\eta_e| < 2.5$ for electrons, $|\eta_\mu| < 2.4$ for muons.
- Transverse momentum of the lepton: $p_T > 20$ GeV for electrons, $p_T > 10$ GeV for muons.

- The four-lepton system includes two pairs of same-flavor opposite-charged leptons are required to form the four-lepton system.

- The pair of leptons with invariant mass closer to mass of Z boson have mass between 40 GeV and 120 GeV, and the other pair have mass between 12 GeV and 120 GeV.

### V.2. Neural Network

The neural network (NN) is used to classify the events into signal and background, trained using the pre-processed data. The NN utilizes feed-forward multi-layer perceptron (MLP) [18] with PyTorch backend [16]. The input features of the NN are the $x$ and $y$ components of momenta, and particle ID of the four-lepton system of the Monte Carlo simulation with invariant mass between 100 GeV and 160 GeV. We use 72% of the data for training, 18% of the data for validation, and 10% of the data for testing. Each lepton is processed individually with three layers of size 32 each. Once the 4 leptons are combined, we have a few more fully-connected layers ($256 \to 64 \to 16 \to 4$) before the final output. The output is yes/no for signal/background.

The NN is trained using the Adam optimizer [12] with a learning rate of $3 \times 10^{-4}$. The loss function is binary cross-entropy [9]. The NN is trained for 100 epochs. The training and validation loss and validation accuracy are shown in Figure 3. The NN is trained to minimize the loss function, and the accuracy is calculated as the number of correct predictions divided by the total number of predictions.

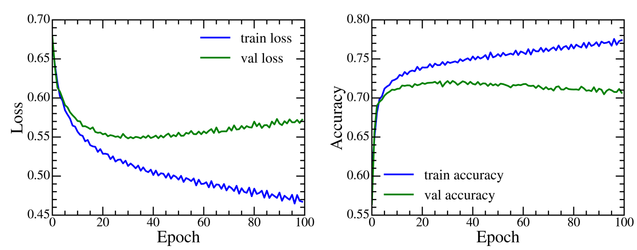


FIG. 3. Training and validation loss and accuracy of the neural network. The loss is calculated using binary cross-entropy. The accuracy is calculated as the number of correct predictions divided by the total number of predictions.

### V.3. Result

After applying the NN and the selection criteria, we obtain the final dataset, shown in Figure 4. The dataset is used to calculate the significance of the excess in signal as a function of mass.

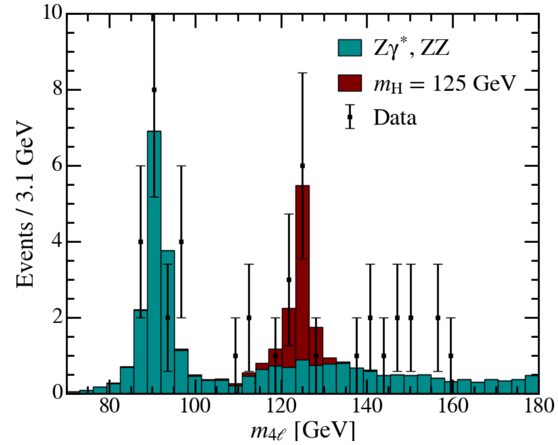


FIG. 4. Final dataset after applying the selection criteria and the neural network. The error bar comes from the standard statistical uncertainty of the data.

## VI. STATISTICAL ANALYSIS

The statistical analysis is performed using the profile likelihood ratio test [? ]. The likelihood function is constructed from the signal and background distributions, and the profile likelihood ratio is used to calculate the significance of the excess in signal. The result is shown in Figure 5.

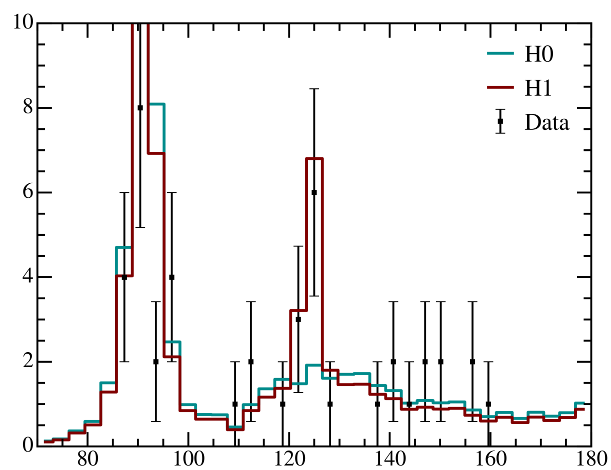


FIG. 5. We have two hypotheses: the null hypothesis (H0) and the alternative hypothesis (H1). The null hypothesis is that there is no signal, and the alternative hypothesis is that there is a signal. The likelihood ratio test statistic is calculated as the ratio of the likelihood of the data under the null hypothesis to the likelihood of the data under the alternative hypothesis. The test statistic is used to calculate the p-value, which is the probability of observing a test statistic as extreme as the one observed, given that the null hypothesis is true.

The significance is calculated using the formula:

$$\text{Significance} = \frac{\mu - \hat{\mu}}{\sigma_{\hat{\mu}}} \tag{1}$$

where $\mu$ is the expected number of signal events, $\hat{\mu}$ is the observed number of signal events, and $\sigma_{\hat{\mu}}$ is the uncertainty in the observed number of signal events. The significance is calculated for each mass point in the range of 100 GeV to 150 GeV, and the results are shown in Figure 6.

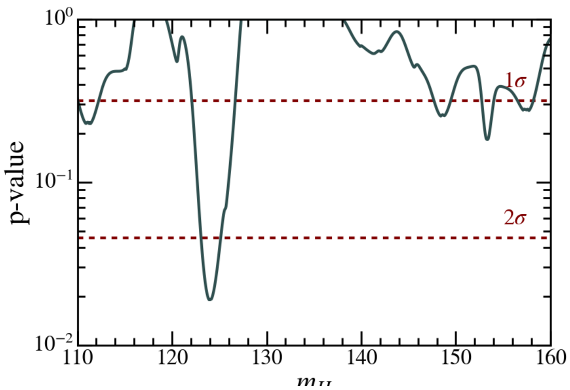


FIG. 6. Significance of the excess in signal as a function of mass. The red line indicates the expected significance, and the blue line indicates the observed significance.

## VII. CONCLUSION

In conclusion, we have reproduced the

## ACKNOWLEDGMENTS

The author gratefully acknowledges their lab partner V. Tran for their invaluable assistance. The author also thanks the 8.13 teaching team for their guidance in the lab. This work was supported by the MIT Department of Physics.


[1] S. Agostinelli et al. Geant4—a simulation toolkit. *Nucl. Instrum. Meth. A*, 506:250–303, 2003.

[2] S. Alekhin et al. The PDF4LHC Working Group Interim Report. 2011.

[3] S. Alioli, P. Nason, C. Oleari, and E. Re. A general framework for implementing nlo calculations in shower monte carlo programs: the powheg box. *JHEP*, 06:043, 2010.

[4] J. Alwall, P. Demin, S. de Visscher, R. Frederix, M. Herquet, F. Maltoni, T. Plehn, D. L. Rainwater, and T. Stelzer. MadGraph/MadEvent v4: The New Web Generation. *JHEP*, 09:028, 2007.

[5] R. D. Ball and others (NNPDF Collaboration). Impact of Heavy Quark Masses on Parton Distributions and LHC Phenomenology. *Nucl. Phys. B*, 849:296–363, 2011.

[6] M. Botje et al. The PDF4LHC Working Group Interim Recommendations. 2011.

[7] S. Chatrchyan et al. Observation of a New Boson at a Mass of 125 GeV with the CMS Experiment at the LHC. *Phys. Lett. B*, 716:30–61, 2012.

[8] C. Collaboration. Cms 2010 collision data, 2014.

[9] I. Goodfellow, Y. Bengio, and A. Courville. *Deep Learning*. MIT Press, 2016.

[10] J. F. Gunion, H. E. Haber, G. L. Kane, and S. Dawson. *The Higgs Hunter's Guide*, volume 80 of *Frontiers in Physics*. Addison-Wesley, 1990.

[11] M. Hu. Higgs to 4l data analysis project, 2020. MIT Junior Lab Spring 2020.

[12] D. P. Kingma and J. Ba. Adam: A method for stochastic optimization. *arXiv preprint arXiv:1412.6980*, 2014.

[13] H.-L. Lai et al. New parton distributions for collider physics. *Phys. Rev. D*, 82:074024, 2010.

[14] MIT Department of Physics. Higgs to 4L Data Analysis Project. Technical report, Massachusetts Institute of Technology, Sep 2020. Dated: September 24, 2020.

[15] Particle Data Group. Status of Higgs Boson Physics. *Prog. Theor. Exp. Phys.*, 2022:083C01, 2022. 2023 update.

[16] A. Paszke, S. Gross, F. Massa, A. Lerer, J. Bradbury, G. Chanan, T. Killeen, Z. Lin, N. Gimelshein, L. Antiga, A. Desmaison, A. Kopf, E. Yang, Z. DeVito, M. Raison, A. Tejani, S. Chilamkurthy, B. Steiner, L. Fang, J. Bai, and S. Chintala. PyTorch: An imperative style, high-performance deep learning library. In H. Wallach, H. Larochelle, A. Beygelzimer, F. d'Alché Buc, E. Fox, and R. Garnett, editors, *Advances in Neural Information Processing Systems 32*, pages 8024–8035. Curran Associates, Inc., 2019.

[17] M. E. Peskin and D. V. Schroeder. *An Introduction to Quantum Field Theory*. Westview Press, Boulder, CO, 1995.

[18] D. E. Rumelhart, G. E. Hinton, and R. J. Williams. Learning representations by back-propagating errors. *Nature*, 323(6088):533–536, 1986.

[19] T. Sjostrand, S. Mrenna, and P. Skands. Pythia 6.4 physics and manual. *JHEP*, 05:026, 2006.

[20] S. Weinberg. *The Quantum theory of fields. Vol. 1: Foundations.* Cambridge University Press, 6 2005.